Cascade Auger transitions of resonantly excited S 1s and Cl 1s holes (photoemission)

1995 J. Phys.: Condens. Matter 7 4385

(http://iopscience.iop.org/0953-8984/7/23/009)

J. Phys.: Condens. Matter 7 (1995) 4385–4394. Printed in the UK

Cascade Auger transitions of resonantly excited S 1s and Cl 1s holes

Teikichi A Sasaki, Yuji Baba, Kenji Yoshii and Hiroyuki Yamamoto

Advanced Science Research Centre, Japan Atomic Energy Research Institute, Tokai-mura, Ibaraki-ken 319-11, Japan

Received 4 October 1994, in final form 6 February 1995

Abstract. Auger decay processes of resonantly excited S 1s holes and Cl 1s holes have been studied for MoS_2 and $SiCl_4$ by photoemission spectroscopy using tunable synchrotron radiation. It is clearly shown that the excited states mainly decay via the $KL_{2,3}L_{2,3}$ and $KL_1L_{2,3}$ spectator Auger transitions. Above the 1s absorption edges, two Auger signals were observed for the $L_{2,3}VV$ Auger transition. Both of them were resonantly enhanced in the vicinity of the 1s absorption edges. The signal of the higher-kinetic-energy side was assigned to the double-ionization satellite originating from the cascade Auger transitions such as $K\underline{L_1}\,\underline{L_{2,3}} \rightarrow (L_1\underline{L_{2,3}}V)\underline{L_{2,3}}VV/V)\underline{L_{2,3}}$ and $K\underline{L_{2,3}}\,\underline{L_{2,3}} \rightarrow (L_{2,3}VV)\underline{L_{2,3}}$. The satellite intensity was analysed for the $S(\underline{L_{2,3}}VV)$ Auger line in $\underline{MoS_2}$, assuming stepwise transitions. The satellite observed was found to have an intensity a third of that expected. The origin of the discrepancy between the experimental and calculated intensities is discussed.

1. Introduction

The decay processes of the resonantly excited states are very important not only for unravelling the mechanism of photodissociation or photon-induced desorption of gaseous molecules but also for understanding the nature of the unoccupied molecular states in solids. Thus the decay channels after resonant excitation have been studied extensively, e.g. for rare gases [1–5] and various molecules [6–12].

In solids, an unoccupied partial density of states within an atomic picture, a degree of degeneration with continuum and a degree of localization of the excited electrons might be discovered [13, 14]. However, the decay process of the resonantly excited states is not completely understood, although much attention has recently been directed towards the Auger decay of the outer core orbitals in transition metals [15, 16], metallic lanthanides [17, 18] and ionic solids [13, 14, 19, 20]. This is because in the resonant excitations of the outer core orbitals it is difficult to separate the spectator Auger spectrum from a participator spectrum. Furthermore, the resulting Auger spectra fall on rather intense and broad structures of the direct photoemission of the valence electrons, which makes the spectrum fairly complicated.

In this work we could distinguish between the spectator and participator Auger transitions by using the deep core orbital excitations. Details of the decay processes via the spectator and participator Auger transitions may be found in reports of related investigations [21–24]. In this report we focus our attention mainly on the cascade Auger transitions.

0953-8984/95/234385+10$19.50

2. Experimental details

Experiments were carried out using monochromated synchrotron radiation from beam line 27A at the Photon Factory in the National Laboratory for High Energy Physics (KEK-PF). The electron spectra were obtained using a VSW Class 100 hemispherical electron energy analyser. The total energy (photon + electron analyser) resolution for most spectra was estimated to be better than 1.3 eV for the S($KL_{2,3}L_{2,3}$) Auger electrons (about 2115 eV) and 1.5 eV for the Cl($KL_{2,3}L_{2,3}$) Auger electrons (about 2380 eV) [21]. For x-ray absorption near-edge structure (XANES) measurements both the total electron yield (TEY) and the partial electron yield (PEY) were recorded by scanning the photon energy.

A molybdenite foil of 10 mm diameter was used for the MoS_2 sample. For the $SiCl_4$ sample, a high-purity solution was degassed and adsorbed on a Cu(100) clean surface at 90 K through a microchannel-plate gas doser. The number of layers in the multi-layered sample was estimated to be about 1200 by means of temperature-programmed desorption measurements. To minimize the effect of charging on the peak width, the surface of the sample was flooded with low-energy electrons during the measurements. The optimum condition of the flood gun, about 20 cm distant from the sample surface, was determined to be 1.6 A for the filament current and less than 0.1 V for the electron energy.

Calibration of the photon energy was performed by reference to the binding energy of the Au $4f_{7/2}$ photoline of metallic Au (purity, 99.99%) as 84.0 eV. Photoinduced decomposition of the samples was checked by recording the photoline shapes of the S 1s region or Cl 1s region and was confirmed to be less than the detection limit. The other details have been given elsewhere [21–25].

3. Results and discussion

3.1. Relative strengths of the Auger decay channels

Figure 1 shows the XANES spectra around the S 1s absorption edge for MoS_2 and the Cl 1s absorption edge for $SiCl_4$. The S 1s edge is attributed to resonant excitations from the S 1s ground state to S 3p* and continuum considering the dipole selection rule (S 3p* indicates antibonding unoccupied molecular states which are mainly composed of the S 3p atomic orbital). On the other hand, peaks A and B of the Cl 1s edge are assigned to the resonant excitations Cl 1s $\rightarrow \sigma^*(a_1)$ and Cl 1s $\rightarrow \sigma^*(t_2)$ where σ^* is the antibonding molecular state of the σ (Si–Cl) bond [26]. Peak C is probably due to the double excitation where the valence electron is excited simultaneously with the Cl 1s $\rightarrow \sigma^*$ excitation and is commonly observed for the XANES spectra of silane derivative compounds [25]. The shaded areas indicate the threshold energies for the normal Auger transitions which were determined from analyses of the resonant Auger electron spectra. Their positions are 2472.1 eV for MoS_2 and 2824.5 eV for $SiCl_4$, which are comparable with 2471.2 eV for the S 1s energy and 2823.3 eV for the Cl 1s energy obtained by XPS with 3314.4 eV photons. The spectral profiles observed are comparable with the previous x-ray absorption spectra of MoS_2 by Ohno *et al* [27] and of $SiCl_4$ by Cicco *et al* [28].

Figure 2 shows the photoemission spectra of MoS_2 which were taken at the on-resonance photon energy (2472.1 eV) and off-resonance photon energies (2466.4 and 2479.8 eV). It is clearly shown that the main lines and their satellites from the $KL_1L_{2,3}$, $KL_{2,3}L_{2,3}$ and $KL_{2,3}V$ Auger transitions are greatly enhanced under the on-resonance condition, while the intensities of the photolines including the valence band region remain almost constant. Similar trends in the spectral shapes were also observed for $SiCl_4$. Peak-area analyses of

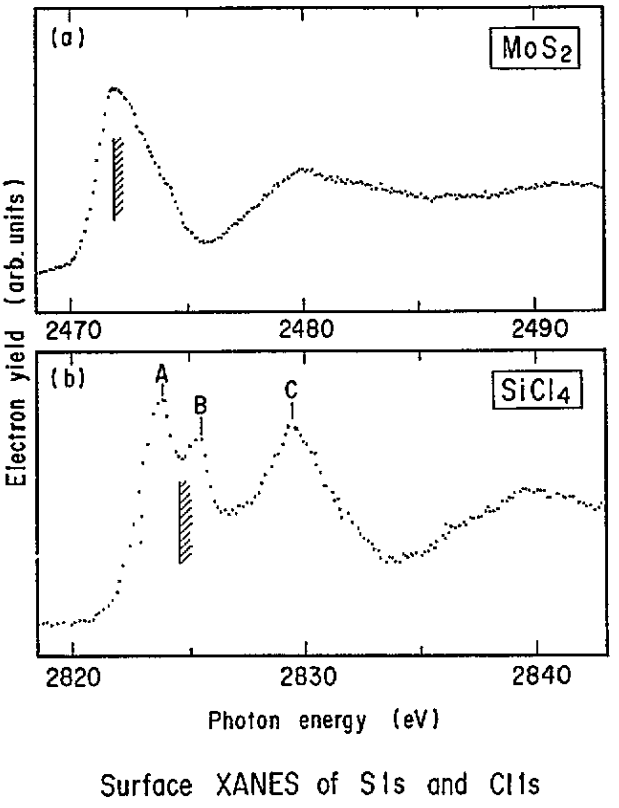

Figure 1. XANES spectra of MoS_2 at the S 1s absorption edge and $SiCl_4$ at the Cl 1s edge. The shaded areas indicate the threshold energy for the normal Auger transitions.

the spectra provide the branching ratio in the decay channel of the S 1s core-hole states. The strengths of the decay channels to various Auger transitions determined are displayed in figure 3 as a function of the photon energy. These are essentially the constant-final-state (CFS) spectra except for a constant-initial-state (CIS) spectrum of the $KL_{2,3}$ participator Auger transition (namely the S 2p photoemission). It is clearly seen that both the $L_{2,3}VV(1)$ and $L_{2,3}VV(2)$ Auger lines are greatly enhanced at the S 1s absorption edge. Their origins will be discussed in detail in section 3.2. The decay channels such as the $KL_{2,3}L_{2,3}$ and $KL_1L_{2,3}$ spectator Auger transitions are also prominent. The lowest curve is for the $KL_{2,3}$ participator Auger transition. It is apparent that the participator Auger transition is not the dominant process (less than 2%) in the Auger decay channels. Similar general trends were obtained for $SiCl_4$ as well.

The relative intensities of the Auger decay channels estimated from the peak-area integration of the CIS and CFS spectra are summarized in table 1 together with the electron kinetic energies of the signals. In this table the backgrounds of the spectra in figure 3 (the contributions mainly from the corresponding normal Auger transitions or from the direct photoemission) were subtracted by means of the linear extrapolation method. It is clearly shown that the excited states decay mainly via the $KL_{2,3}L_{2,3}$ and $KL_1L_{2,3}$ spectator Auger transitions. In the case of $SiCl_4$, decay components of the Cl 1s hole states were found to be very sensitive to the exciting photon energy, and the spectral analyses are now in progress.

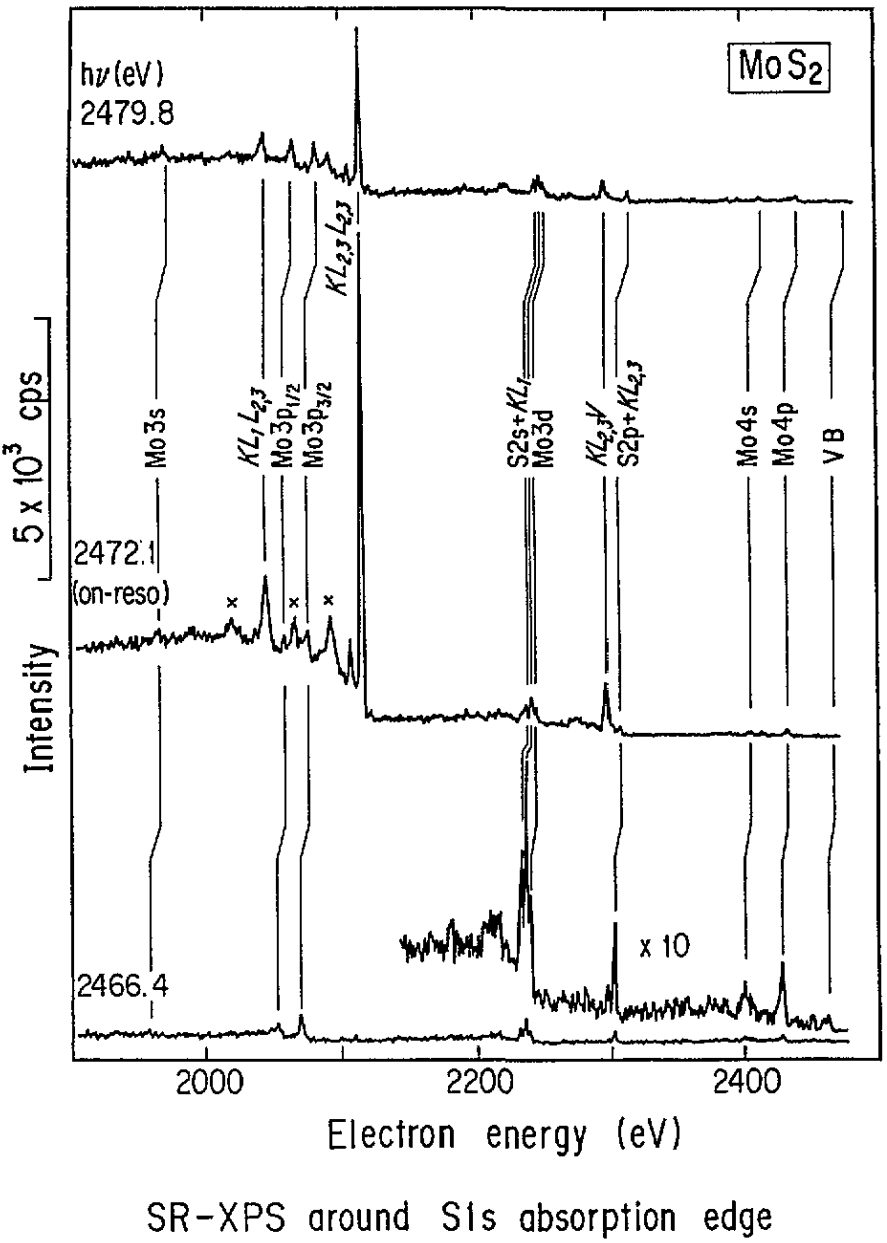

Figure 2. Photoemission wide-scan spectra for MoS_2 taken under on-resonance condition (2472.1 eV) and off-resonance conditions (2466.4 and 2479.8 eV): —×—, lines where the final-state terms are different from those of the main lines whose final terms are assigned to $^1D_2$ and $^1P_1$ for the $KL_{2,3}L_{2,3}$ and $KL_1L_{2,3}$ Auger transitions, respectively [29].

3.2. High-energy satellite of the $L_{2,3}VV$ Auger line

Great enhancements in the signal intensities of the two Auger lines $L_{2,3}VV(1)$ and $L_{2,3}VV(2)$ in figure 3 suggest the occurrences of cascade Auger transitions. In the framework of the resonant excitations, two types of the decay channel are considered: one is via non-radiative

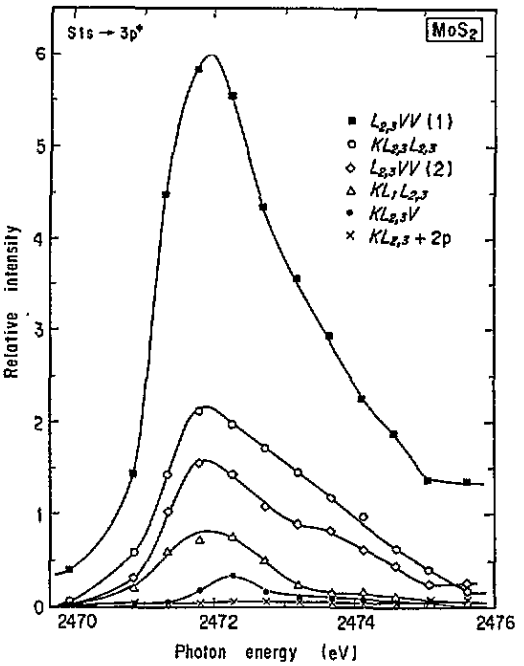

Figure 3. Decay channels to various Auger transitions in MoS_2 against the photon energy. The curves correspond to CFS spectra for the $KL_1L_{2,3}$, $KL_{2,3}L_{2,3}$, $KL_{2,3}V$, $L_{2,3}VV(1)$ and $L_{2,3}VV(2)$ Auger transitions, and CIS spectrum for the $KL_{2,3}$ Auger transition.

Table 1. Peak assignments of the transitions, electron kinetic energies and relative spectral intensities in MoS_2. The relative intensities are estimated from the CFS and CIS spectra in figure 3 and normalized to that of the $KL_{2,3}L_{2,3}$ spectator Auger line.

Transition	Electron energy (eV)	Relative intensity
$KL_1L_{2,3}$	≃2047	0.29
$KL_{2,3}L_{2,3}$	≃2116	1.0
$KL_{2,3}V$	≃2285	0.09
$KL_{2,3}$	2298.8[a]	0.04
$L_{2,3}VV(1)$	148	2.17
$L_{2,3}VV(2)$	167	0.65

[a] Same as S 2p photoemission energy. This is the value at a photon energy of 2472.1 eV.

decays such as the spectator Auger transitions or the participator Auger transitions, and the other via radiative decay such as the luminescent x-ray emission. Figures 4 and 5 show spectral evolutions of the $S(L_{2,3}VV)$ Auger energy region of MoS_2 and the $Cl(L_{2,3}VV)$ Auger energy region of $SiCl_4$, respectively. Since no Auger lines other than the $L_{2,3}VV$ line should exist in these regions, both peaks in each figure are attributed to the $L_{2,3}VV$ Auger transition.

In the following we focus our attention mainly on the observations for MoS_2, because almost the same conclusions could be deduced from the observations for $SiCl_4$. A 147 eV peak, $L_{2,3}VV(1)$, in the spectrum in figure 4 with photons of 2467.9 eV which is far below the S 1s absorption edge is assigned to the $L_{2,3}VV$ normal Auger transition itself and the

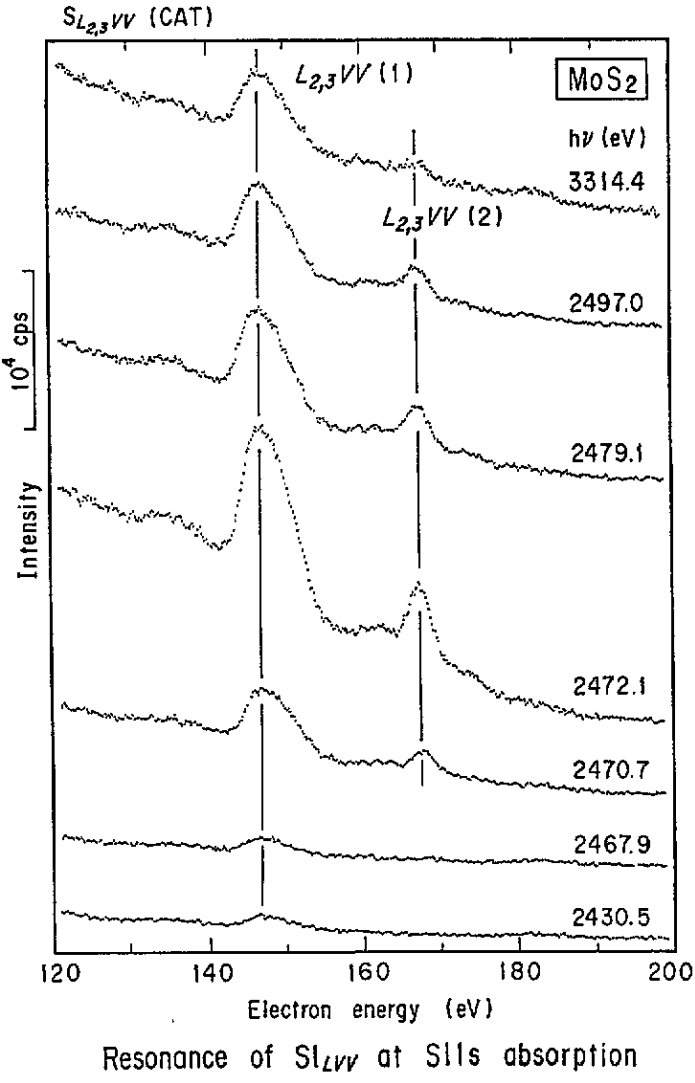

Figure 4. Evolution of the $S(L_{2,3}VV)$ Auger electron spectra for MoS_2.

$L_1L_{2,3}V$ Coster–Kronig transition followed by the $L_{2,3}VV$ transition. The intensity of this peak increases appreciably far beyond the absorption edge, as seen in the spectrum with 3314.4 eV photons. This is due to an additional contribution mainly from the $KL_{2,3}L_{2,3}$ normal Auger transition followed by the $L_{2,3}VV$ Auger transition.

The origin of the high-energy satellite such as the $L_{2,3}VV(2)$ Auger line has been extensively discussed [30–34] and conclusively attributed to double ionization [34]. In addition Fuggle [34] has observed that satellite intensity of the Mg ($L_{2,3}VV(2)$) Auger line (of kinetic energy 61 eV) from solid Mg has an intensity a third of that of the main line using Al Kα radiation (1486.6 eV) for the excitation. In the case of the S 1s excitation and the subsequent decay processes, the S 2p electrons and/or valence electrons would be successively captured by the resulting L_1 and/or $L_{2,3}$ holes. The energy separation between

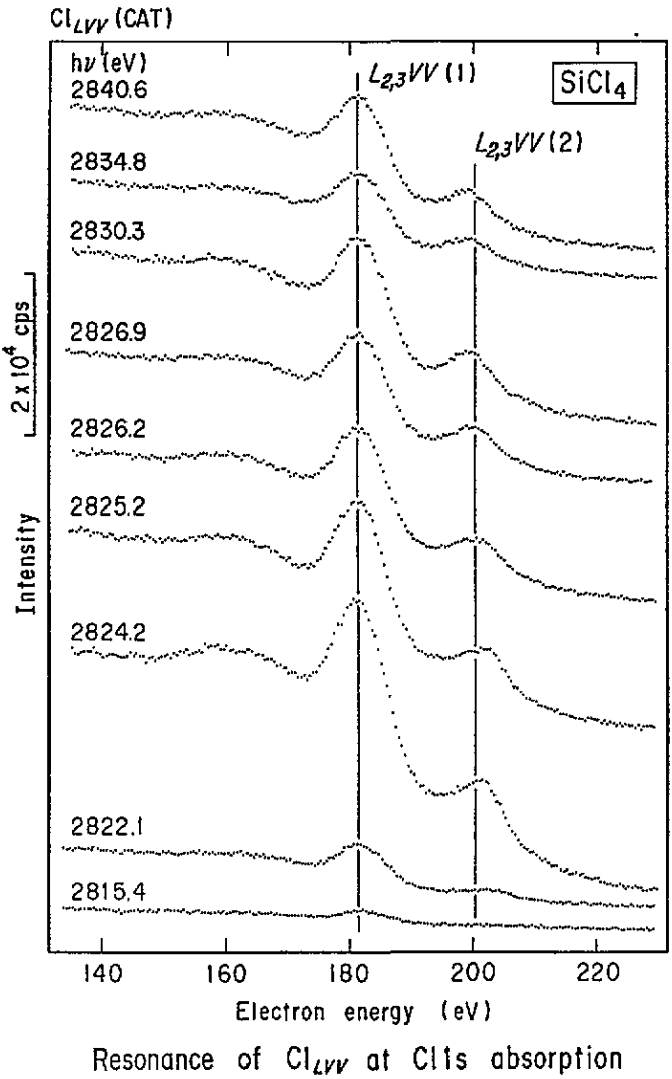

Figure 5. Evolution of the Cl($L_{2,3}VV$) Auger electron spectra for $SiCl_4$.

the $L_{2,3}VV(1)$ Auger line and $L_{2,3}VV(2)$ Auger line may be caused by the effect of an additional vacancy on the nuclear screening experienced by the S 2p electrons and valence electrons. The resonantly enhanced spectra in figures 4 and 5 are more well resolved than those in previous work obtained by the conventional x-ray sources [30–34], which allows us to evaluate the satellite quantitatively.

Table 2 shows the successive decay processes of the core holes and the contributions of the decay steps to the $L_{2,3}VV(1)$ and $L_{2,3}VV(2)$ Auger lines. Since the peak intensities of the signals corresponding to such decay processes as the KL_1L_1, KL_1V, L_1VV Auger transitions, etc, were so weak compared with that of the $KL_{2,3}L_{2,3}$ Auger transition, their contributions are omitted. Then the ratio R of the intensity of satellite to that of the main line can be approximated as

Table 2. Decay processes, relative frequencies of the $L_{2,3}VV$ Auger lines to which the decay processes of the S 1s hole in MoS_2 are contributed. The underlined L represents an L orbital with an electron hole.

Decay processes: 1st step	Subsequent steps	Contributed line	Relative frequency
K(1s) photoabsorption			
$\underline{KL_1L_{2,3}}$	$(L_1\underline{L_{2,3}}V)\underline{L_{2,3}}$		
	$(L_{2,3}VV/V)\underline{L_{2,3}}$	$L_{2,3}VV(2)$	1.87
	$(VV/V)L_{2,3}VV$	$L_{2,3}VV(1)$	1.87
$\underline{KL_{2,3}L_{2,3}}$	$(L_{2,3}VV)\underline{L_{2,3}}$	$L_{2,3}VV(2)$	6.41
	$(VV)L_{2,3}VV$	$L_{2,3}VV(1)$	6.41
$\underline{KL_{2,3}V}$	$(L_{2,3}VV)V$	$L_{2,3}VV(1)$	0.59
$\underline{KL_{2,3}}$ participator	$L_{2,3}VV$	$L_{2,3}VV(1)$	0.30
$\underline{KL_{2,3}}$ luminescent	$L_{2,3}VV$	$L_{2,3}VV(1)$	0.77
$L_1(2s)$ ionization			
$L_1\underline{L_{2,3}V}$	$L_{2,3}VV$	$L_{2,3}VV(1)$	0.58
$L_{2,3}(2p)$ ionization			
$L_{2,3}VV$		$L_{2,3}VV(1)$	0.44

$$R \simeq [N(KL_1L_{2,3}) + N(KL_{2,3}L_{2,3})]/[N(KL_1L_{2,3}) + N(KL_{2,3}L_{2,3}) + N(KL_{2,3}V) + N^{P}(KL_{2,3}) + N^{I}(KL_{2,3}) + N(L_1L_{2,3}V) + N(L_{2,3}VV)].$$

Here N is frequency of the corresponding Auger transition, and N^{P} and N^{I} indicate the frequencies of the participator Auger transition and of luminescent process, respectively. Employing the relative intensities in table 1 to derive the relative frequencies of the Auger transitions, this simplifies to

$$0.91a_K\sigma_i(K)/[a_K\sigma_i(K) + \omega_K\sigma_i(K) + f_L\sigma_i(L_1) + a_L\sigma_i(L_{2,3})].$$

Here a, ω, f and σ_i are the Auger yield, luminescent yield, Coster–Kronig yield and photoionization cross section of the corresponding core holes, respectively. It should be also noted that $N(KL_{2,3}L_{2,3})$ was replaced by $0.70a_K\sigma_i(K)$, because the relative intensity for the $KL_{2,3}L_{2,3}$ process is 70% of the sum for those for the $KL_1L_{2,3}$, $KL_{2,3}L_{2,3}$, $KL_{2,3}V$ and $KL_{2,3}$ processes. For the $KL_{2,3}$ luminescent process and the $L_1L_{2,3}V$ Coster–Kronig process, f_L and a_L were taken to be 0.078 and 0.944, respectively [35]. Furthermore the $KL_{2,3}$ luminescent process is inevitably followed by the $L_{2,3}VV$ Auger transition, because

there is no branching to luminescent $L_{2,3}V$ (i.e. Lα) emission in the decay of the $L_{2,3}$ hole [35]. Assuming that the photoionization cross sections at about 2472 eV are 9.99×10^{-20} cm^2 for σ_i(K), 0.616×10^{-20} cm^2 for $\sigma_i(L_1)$ and 0.441×10^{-20} cm^2 for $\sigma_i(L_{2,3})$ [36], we obtain the relative frequencies given in the last column of table 2 and thus 0.76 for the R-value. On the other hand, the experimental ratio of the intensity of the satellite to that of the main line can be estimated to be 0.30 from the relative intensities for the $L_{2,3}VV(1)$ and $L_{2,3}VV(2)$ processes in table 1. Thus the calculated satellite intensity is significantly larger than the observed value.

In the calculations it is expected that the R-value should not deviate excessively from 1, because both the $L_{2,3}VV(1)$ and the $L_{2,3}VV$ Auger transitions are dominantly contributed by the $KL_1L_{2,3}$ and $KL_{2,3}L_{2,3}$ Auger transitions, as seen in table 2. The discrepancy between the calculated and experimental ratios is probably due to the very fast relaxation of the double-core-hole states. It is considered that in the condensed phase some part of the double core holes, denoted $\underline{KL_{2,3}}\,\underline{L_{2,3}}$ for example in table 2, collapses via simultaneous neutralizations by two electrons in the valence band, which may cause both the decrease in the satellite intensity and the increase in the main-line intensity. These may occur for the same reason that the observed satellite intensity of the $Mg(L_{2,3}VV)$ Auger line has an intensity a third of that expected [34]. For a full understanding of double ionization in solids, detailed theoretical treatments based on the dynamics of the core-hole decay are required.

4. Conclusion

Auger decay channels after the resonant $1s \rightarrow 3p^*$ excitation in MoS_2 and $SiCl_4$ have been studied by photoemission spectroscopy using synchrotron radiation. It was observed that the main channels are through the $KL_{2,3}L_{2,3}$ and $KL_1L_{2,3}$ spectator Auger transitions. Above the threshold energy of the core hole, two Auger signals were observed for the $L_{2,3}VV$ Auger transition. One of them was assigned to the double-ionization satellite originating from cascade Auger transitions such as $\underline{KL_1}\,\underline{L_{2,3}} \rightarrow (L_1\underline{L_{2,3}}V)\underline{L_{2,3}} \rightarrow (L_{2,3}VV/V)\underline{L_{2,3}}$ and $\underline{KL_{2,3}}\,\underline{L_{2,3}} \rightarrow (L_{2,3}VV)\underline{L_{2,3}}$. The observed satellite of the $S(\underline{L_{2,3}}\underline{V}\underline{V})$ Auger line in MoS_2 was found to have an intensity about a third of that expected. The origin of the discrepancy between the experimental and calculated intensities was discussed and was attributed to collapses of the double core holes via simultaneous neutralizations by electrons in the valence band.

Acknowledgments

The staff of KEK-PF are greatly acknowledged for their assistance throughout the experiment. The authors wish to thank Dr A Yokoya, Mr H Konishi and Mr H Motohashi of the Japan Atomic Energy Research Institute for their help in the conditioning of the BL-27A. This work was done with the approval of the Photon Factory Program Advisory Committee (PF-PAC 93G316).

References

[1] Armen G B, Åberg T, Levin J C, Crasemann B, Chen M H, Ice G E and Brown G S 1985 *Phys. Rev. Lett.* 54 1142

[2] Becker U, Prescher T, Schmidt E, Sonntag B and Wetzel H-E 1986 *Phys. Rev.* A **33** 3891
[3] Aksela H, Aksela S, Pulkkinen H and Yagishita A 1989 *Phys. Rev.* A **40** 6275
[4] Raven E von, Meyerm M, Pahler M and Sonntag B 1990 *J. Electron Spectrosc. Relat. Phenom.* **52** 677
[5] Aksela H, Aksela S, Mantykentta A, Tulkki J, Shigemasa E, Yagishita A and Furusawa Y 1992 *Phys. Scr.* T **41** 113
[6] Aksela S, Tan K H, Aksela H and Bancroft G M 1986 *Phys. Rev.* A **33** 258
[7] Wurth W, Schneider C, Treichler R, Treichler E, Menzel D and Umbach E 1988 *Phys. Rev.* B **37** 8725
[8] Aksela S, Sairanen O-P, Aksela H, Bancroft G M and Tan K H 1988 *Phys. Rev.* A **37** 2934
[9] Bancroft G M, Tan K H, Sairanen O-P, Aksela S and Aksela H 1990 *Phys. Rev.* A **41** 3717
[10] Aksela H, Aksela S, Sairanen O-P and Kivimäki A 1992 *Phys. Scr.* T **41** 122
[11] Wurth W, Feulner P and Menzel D 1992 *Phys. Scr.* T **41** 213
[12] Kivimäki A, Broto A N de, Aksela S, Aksela H, Sairanen O-P, Ausmees A, Osborne S, Dantas L B and Svensson S 1993 *Phys. Rev. Lett.* **71** 4307
[13] Kikas A, Ausmees A, Elango M, Nõmmiste E and Ruus R 1992 *Phys. Scr.* T **41** 237
[14] Kamada M, Aita O, Ichikawa K, Okusawa M and Tsutsumi K 1992 *Phys. Rev.* B **45** 12 725
[15] Sarma D D, Carbone C, Sen P, Cimino R and Gudat W 1989 *Phys. Rev. Lett.* **63** 656
[16] Sorma D D, Cimino R, Carbone C, Sen P, Barman S R and Gudat W 1992 *Phys. Scr.* T **41** 187
[17] Sairanen O-P, Aksela S and Kivimäki A 1991 *J. Phys.: Condens. Matter* **3** 8707
[18] Sairanen O-P 1992 *Phys. Scr.* T **41** 163
[19] Ichikawa K, Aita O, Aoki K, Kamada M and Tsutsumi K 1992 *Phys. Rev.* B **45** 3227
[20] Elango M, Ausmees A, Kikas A, Nõmmiste E, Ruus R, Saar A, Acker J F van, Anderesen J N, Nyholm R and Martinson I 1993 *Phys. Rev.* B **47** 11 736
[21] Baba Y, Sasaki T A and Yamamoto H 1994 *Phys. Rev.* B **49** 709
[22] Sasaki T A, Baba Y, Yoshii K, Yamamoto H and Nakatani T 1994 *Phys. Rev.* B **50** 15 519
[23] Sasaki T A, Baba Y, Yoshii K and Yamamoto H 1995 *J. Phys.: Condens. Matter* **7** 463
[24] Yoshii K, Baba Y and Sasaki T A 1995 *J. Electron Spectrosc. Relat. Phenom.* at press
[25] Baba Y, Yoshii K, Yamamoto H and Sasaki T A 1995 *J. Phys.: Condens. Matter* **7** 1991
[26] Ishikawa H, Fujima K, Adachi H, Miyauchi E and Fujii T 1991 *J. Chem. Phys.* **94** 6740
[27] Ohno Y, Hirama K, Nakai S, Sugiura C, Okada S 1983 *Phys. Rev.* B **27** 3881; 1983 *J. Phys. C: Solid State Phys.* **16** 6695
[28] Cicco Di A, Stizza S, Filliponi A, Boscherini F and Mobilio S 1992 *J. Phys. B: At. Mol. Opt. Phys.* **25** 2309
[29] Asplund L, Kelfve P, Blomster B, Siegbahn H and Siegbahn K 1977 *Phys. Scr.* **16** 273
[30] Hanson W F and Arakawa E T 1972 *Z. Phys.* **251** 271
[31] Guennou H, Dufour G and Bonnelle C 1974 *Surf. Sci.* **41** 547
[32] Salmeron M, Baro A M and Rojo J M 1974 *Surf. Sci.* **41** 11
[33] Lofgren H and Wallden L 1973 *Solid State Commun.* **12** 19
[34] Fuggle J C 1977 *J. Phys. F: Met. Phys.* **7** L81
[35] Krause M O 1979 *J. Phys. Chem. Ref. Data* **8** 307 and references therein
[36] Scofield J H 1973 *Lawrence Livermore Laboratory Report* UCRL-51326